JOURNAL OF SOLID STATE CHEMISTRY 48, 309–317 (1983)

The Structures of Lithium Inserted Metal Oxides: $Li_2FeV_3O_8$

R. J. CAVA, A. SANTORO,* D. W. MURPHY, S. ZAHURAK, AND R. S. ROTH*

*Bell Laboratories, 600 Mountain Avenue, Murray Hill, New Jersey 07974, and *National Bureau of Standards, Washington, D.C. 20234*

Received November 24, 1982; in revised form February 25, 1983

Neutron diffraction powder profile analysis has been used to determine the structure of $Li_2FeV_3O_8$. The compound is prepared from FeV_3O_8, which has the VO_2(B) structure type, by a lithium insertion reaction employing *n*-BuLi. Only minimal distortion of the host lattice occurs on Li insertion. The Li ions occupy five coordinate square pyramidal sites with an average Li–O bond distance of 2.04 Å. These five coordinate sites occur commonly in the capped perovskite cavities of crystallographic shear structures based on ReO_3.

Compounds which can reversibly incorporate lithium at room temperature are of interest due to their potential use as positive electrode materials in secondary batteries (*1*). Of the framework structure transition metal oxides, those with the rutile structure and ReO_3 based shear structures (such as V_6O_{13}) have been the subject of many studies. The structures of Li inserted metal oxides are of interest both to determine the preferred Li coordination geometries and the changes in the host lattice during insertion. The unavailability of single crystals of the lithium inserted metal oxides makes conventional structural characterization techniques nonapplicable. The reported structures of Li insertion compounds obtained from ReO_3, ($LiReO_3$ and Li_2ReO_3) and $LiMoO_2$ and the high temperature lithium bronze $Li_{0.36}WO_3$ were determined by neutron powder diffraction or powder profile analysis (NDPPA) (*2–4*).

In $LiMoO_2$, $LiReO_3$, and Li_2ReO_3, the inserted Li ions occupy LiO_6 octahedra, some of which are severely distorted. Such octahedral sites are already present but vacant in the MoO_2 rutile structure, but in ReO_3 (which is made exclusively of corner shared ReO_6 octahedra) they are created on lithium insertion by an extensive twist to a structure of the PdF_3 type. In a large class of Li insertable host structures based on shear derivitives of the ReO_3 type structure, octahedrally coordinated interstitial sites are not present and the lattice parameters do not change radically on lithium insertion, implying that the crystallographic shear (*CS*) may prevent the distortion of the host lattice to produce such octahedral sites. Lithium therefore is not likely to occupy octahedral environments in this type of compound, which includes important materials such as V_6O_{13}.

We have chosen lithium inserted FeV_3O_8, $Li_2FeV_3O_8$ as a prototype of the ReO_3 derived *CS* compounds. This report elaborates on a preliminary discussion published elsewhere (*5, 6*). The structure of FeV_3O_8 is that of a (2,2) shear of ReO_3, also found in VO_2(B), TiO_2(B), and $AlNbO_4$, and contains one dimensional channels formed by interconnected perovskite-like

0022-4596/83 $3.00

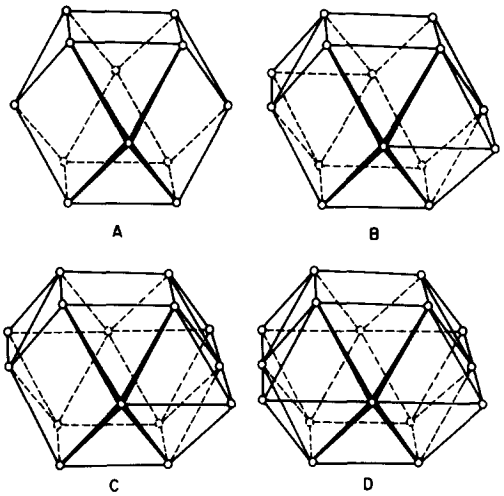

FIG. 1. Perovskite related cavities in ReO_3 and various vanadium oxide crystallographic shear structures. (A) ReO_3 cavity, (B) Bicapped cavity found in V_2O_5, (C) Tricapped cavity found in V_6O_{13}, (D) Tetra-capped cavity found in VO_2(B).

cavities in the shape of four-capped cubo-octahedra. The cavity is illustrated in Fig. 1, and is compared to those in ReO_3 and other *CS* structures. The channels are of the same dimension as those in V_6O_{13}, and the overall structure is that of V_6O_{13} with one plane of corner shared octahedra missing. The formation of $Li_{.75}VO_2$(B) by Li insertion and similar results for TiO_2(B) (*7*) have been reported. This stoichiometry would require three lithium ions per perovskite-like cavity. We have been unable to prepare either of these compositions with diffraction patterns suitable for NDPPA. This may be due to the thermal instability of TiO_2(B) and VO_2(B) which prevents crystal growth during their synthesis. Our NDPPA results on $Li_2FeV_3O_8$ indicate that the two Li per perovskite-like cavity are accommodated in five-coordinate LiO_5 polyhedra, with minimal distortion of the FeV_3O_8 structural framework.

Procedure and Results

The mixed metal compound $Fe_{1+x}V_{3-x}O_8$ ($x \approx 0.06$) was grown by Muller *et al.* (*8*) from a molten vanadium oxide flux. We have determined that good quality polycrystalline powder samples can be prepared from stoichiometric mixtures of $FeVO_4$ and VO_2 at 700°C. Reaction of FeV_3O_8 with *n*-BuLi at room temperature results in stoichiometries of $Li_xFeV_3O_8$ ($x \gtrsim 1.5$). Treatment at 50°C with *n*-BuLi gives $x \lesssim 2.3$. Delithiation with iodine removes only ~2.0 equivalents of Li after treatment at 50°C (~1.5 at room temperature). Because of this discrepancy and the NDPPA results it is probable that the Li in excess of two is present in a second phase. Studies of the $Li_xFeV_3O_8$ system using x values from delithiation reactions calculated on the basis of the limiting formula $Li_2FeV_3O_8$ show single phase regions for $0 < x \lesssim 0.9$ and $1.75 \lesssim x \lesssim 2.0$ with a two phase region for intermediate values of x. The lattice parameters (determined by X-ray diffraction) and the X-ray powder diffraction pattern for $Li_2FeV_3O_8$ are given in Table I.

TABLE I

X-RAY POWDER DIFFRACTION PATTERN AND MONOCLINIC UNIT CELL PARAMETERS FOR $Li_2FeV_3O_8$

h	k	l	d_{calc}	d_{obs}	I/I_0
0	0	1	6.176	6.181	80
2	0	0	5.716	5.724	40
−2	0	1	4.993	4.997	10
1	1	0	3.691	3.700	40
0	0	2	3.088	3.087	100
−4	0	1	2.946	2.943	30
4	0	0	2.858	2.857	10
3	1	0	2.725	2.726	20
−4	0	2	2.496	2.495	10
4	0	1	2.344	2.344	10
0	0	3	2.059	2.059	80
−6	0	1	1.994	1.995	30
−3	2	1	1.733	1.733	10
6	0	1	1.686	1.685	10
4	0	3	1.477	1.477	10

Note: X-ray cell parameters (Å): $a = 11.963(3)$, $b = 3.899(2)$, $c = 6.464(2)$, $\beta = 107.5(3)°$.

TABLE II

EXPERIMENTAL CONDITIONS USED TO COLLECT THE NEUTRON POWDER INTENSITY DATA FOR $Li_2FeV_3O_8$

Monochromatic beam:	reflection 220 of a Cu monochromator	
Wavelength:	1.5416(3) Å	
Horizontal divergences:	(a) in-pile collimator	10′ arc
	(b) monochromatic beam collimator:	20′ arc
	(c) diffracted beam collimator:	10′ arc
Monochromator mosaic spread:	~15′ arc	
Sample container:	vanadium can ~10 mm in diameter	
Angular ranges scanned by each detector:	10–40, 30–60, 50–80, 70–100, 90–120	
Angular step:	0.05°	

Neutron diffraction measurements were performed on the high resolution five counter powder diffractometer at the NBS Reactor, with neutrons of wavelength 1.5416(3) Å. The experimental conditions used to collect the data are presented in Table II. The powder profile refinement was performed using the Rietveld program (*9*) adapted to the five detector diffractometer design and modified to allow the refinement of background intensity (*10*). The program has been further modified to describe non-Gaussian profiles with the Pearson type VII distribution, which allows the line shape to be varied continuously from Gaussian to Lorentzian by changing one additional profile parameter. This method, described in detail elsewhere (*11*), was critical in the refinements of the structure.

The neutron scattering amplitudes employed were $b(\mathrm{Li}) = -0.214$, $b(\mathrm{V}) = -0.038$, $b(\mathrm{Fe}) = 0.95$, and $b(\mathrm{O}) = 0.58$ ($\times 10^{-12}$ cm) (*12*). Initial lattice parameters were obtained by a least-squares fit to the X-ray diffraction data. Approximate values of the background parameters were obtained at positions in the pattern free from diffraction effects. Several regions in the powder pattern, of length 1 to 2° in 2θ, were omitted from the refinement due to the presence of diffracted intensities from a small fraction of impurity phase. In the refinement of the structural models, all structural, lattice, and profile parameters were refined simultaneously. Refinements were terminated when in two successive cycles the factor R_w (see Table III) varied by less than one part in a thousand. In the final refinement 19 profile and 17 structural parameters were varied.

In the initial refinements of the structure, only the atoms of the FeV_3O_8 host structure were included. These were placed in the positions 4*i* (x,0,z) of space group *C*2/*m*, with the coordinates determined for FeV_3O_8 by Muller *et al.* (*8*) (two formula units per unit cell). Difference Fourier synthesis, employing the observed and calculated structure factors extracted from the

TABLE III

STRUCTURE OF $Li_2FeV_3O_8$ (SPACE GROUP: *C*2/*m*, $Z = 2$, ATOMS IN POSITION 4*i*)

Atom	X	Y	Z	$B(A^2)$
Li	0.951(2)	0.0	0.659(3)	3.4(3)
*M*1	0.278(2)	0.0	0.585(4)	0.0(1)
*M*2	0.3968(7)	0.0	0.314(1)	0.0(1)
O1	0.3494(4)	0.0	0.9954(8)	0.59(3)
O2	0.2287(4)	0.0	0.3416(8)	0.59(3)
O3	0.4424(5)	0.0	0.6413(7)	0.59(3)
O4	0.1207(4)	0.0	0.6840(7)	0.59(3)
	$N_1^{Fe} = 0.0625$		$N_2^{Fe} = 0.1875$	
	$N_1^{V} = 0.4375$		$N_2^{V} = 0.3125$	

Note: $R_N = 9.15\%$, $R_p = 5.84\%$, $R_w = 7.77\%$, $R_E = 3.45\%$.

$$R_N = \frac{\Sigma|I(\mathrm{obs}) - I(\mathrm{calc})|}{\Sigma I(\mathrm{obs})}$$

$$R_p = \frac{\Sigma|y(\mathrm{obs}) - y(\mathrm{calc})|}{\Sigma y(\mathrm{obs})}$$

$$R_w = \left\{\frac{\Sigma w[y(\mathrm{obs}) - y(\mathrm{calc})]^2}{\Sigma w[y(\mathrm{obs})]^2}\right\}^{1/2}$$

$$R_E = \left\{\frac{N - P + C}{\Sigma w[y(\mathrm{obs})]^2}\right\}^{1/2}$$

where N = number of independent observations, P = number of parameters, C = number of constraints, y = counts at angle 2θ, I = integrated Bragg intensities, and w = weights.

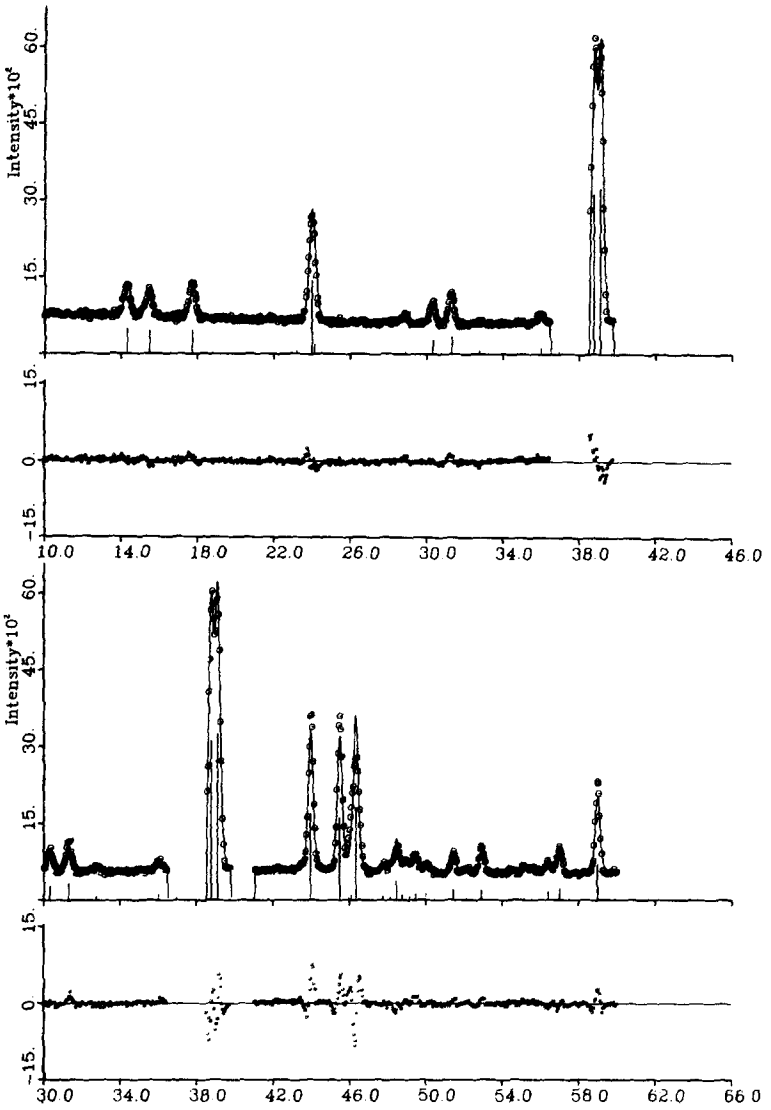

FIG. 2. Observed and calculated powder neutron diffraction profile intensities for $Li_2FeV_3O_8$. Under the profile for each of the five detectors, plotted on the same scale, are the differences between the observed and calculated profiles.

profile fitting procedure, were employed to locate the positions of the inserted lithium atoms. Such positions are clearly visible as regions of negative scattering density in the difference map. The four Li per unit cell are also located in a position of type 4*i* (*x*,0,*z*). As reported by Muller *et al.*, the iron and vanadium in the host structure are disordered over two octahedral metal positions. The disorder can be described with the following chemical and structural constraints for the occupancies of N_1^X of the metal sites *M*1 and *M*2:

$$\begin{aligned} M1: &\quad N_1^{Fe} + N_1^{V} = 0.5 \\ M2: &\quad N_2^{Fe} + N_2^{V} = 0.5 \\ \text{Fe balance:} &\quad N_1^{Fe} + N_2^{Fe} = 0.25 \\ \text{V balance:} &\quad N_1^{V} + N_2^{V} = 0.75 \end{aligned}$$

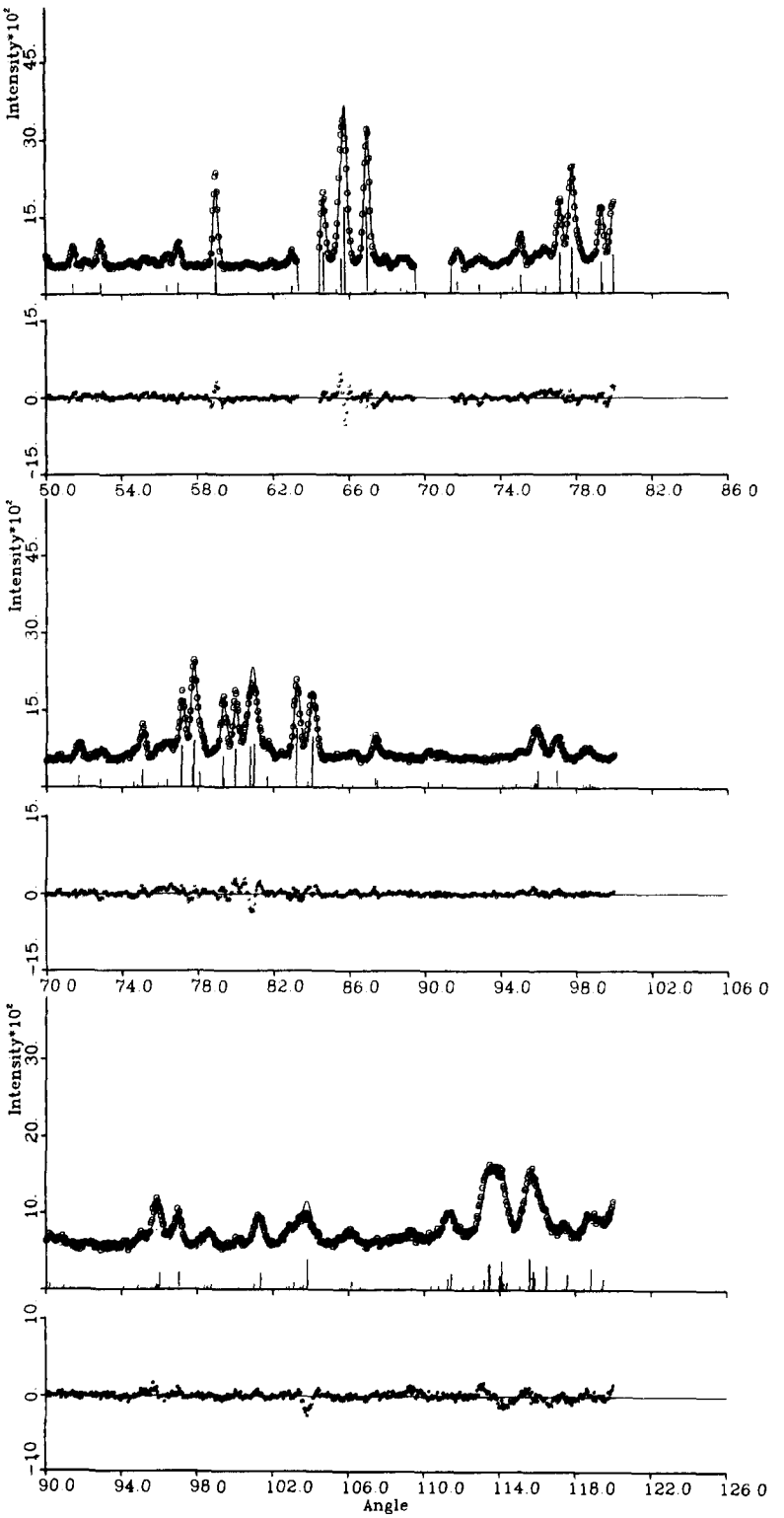

FIG. 2—*Continued.*

where the sum of the occupancies for each site is given by the multiplicity four of the site of type $(x,0,z)$, divided by the multiplicity eight of the general position. Refinement of the occupancy parameter N_2^{Fe} showed that the vanadium/iron distribution in our host material was in excellent agreement with that published by Muller *et al.* The fact that the $M1$ site is occupied almost exclusively by vanadium ($N_1^V = 0.4375$, $N_1^{Fe} = 0.0625$) results in a very small contribution of that site to the structure factors, making characterization of the $M1$ metal atoms difficult by means of neutron diffraction. The Fe/V site occupancies were therefore fixed at the values determined by Muller *et al.*, and the thermal parameters for the cations in the sites $M1$ and $M2$ of the host structure were constrained to be equal. The thermal parameters of the four independent oxygen atoms were also constrained to be equal. Such constraints on the thermal parameters are somewhat artificial but are not likely to be violated significantly in a compound of this type, and do not affect in any way the determination of the positional parameters.

The structural parameters for the final model of $Li_2FeV_3O_8$ are given in Table III, as are the agreement factors for the Bragg intensities (R_N), the profile and weighted profile fits (R_p and R_w), and the agreement expected solely from statistics (R_E). As for the case of the lithium insertion compounds $LiReO_3$ and Li_2ReO_3, the diffraction line profiles for $Li_2FeV_3O_8$ are not strictly Gaussian. For well-crystallized materials, diffracted line profiles are Gaussian to an excellent approximation under the experimental conditions employed. The deviation from Gaussian for the lithium insertion compounds may be due to particle size distribution or strain. The line profiles for $Li_2FeV_3O_8$ were approximated by the Pearson type VII distribution, with $m = 3$. Observed and calculated profile intensities are shown in Fig. 2.

The FeV_3O_8 host structure has undergone only minimal distortion on lithium insertion. Figure 3 presents a view of the structure down the monoclinic b axis in which the ReO_3 type blocks and extensive edge sharing of the VO_2(B) type structure are evident. Host lattice metal ion octahedra are outlined. The large perovskite-like cavities occur along the unit cell edges, and are occupied by two lithium ions. The lithium ions are coordinated to three oxygen ions in the same plane perpendicular to b and two oxygen ions $\pm\frac{1}{2}b$ away, in an LiO_5 polyhedron which is best described as a square pyramid. The coordination geometry is shown in detail in Fig. 4.

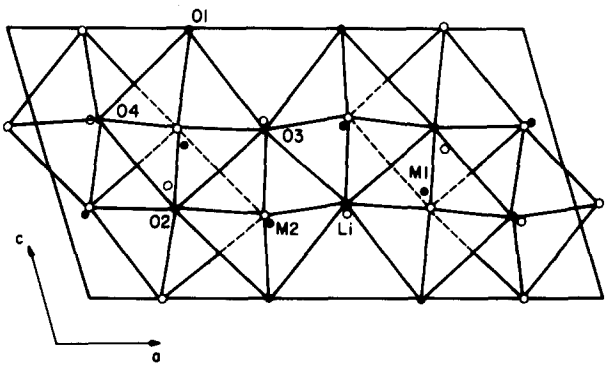

FIG. 3. The structure of $Li_2FeV_3O_8$ in projection down the monoclinic b axis. Closed circles are atoms at $y = 0$ and open circles are atoms at $y = \frac{1}{2}$. The metal–oxygen octahedra of the FeV_3O_8 host lattice are outlined.

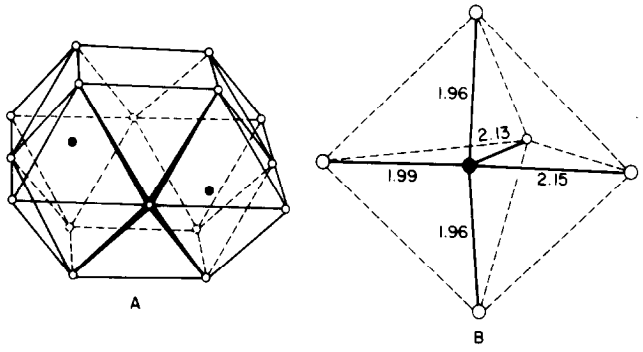

FIG. 4. (A) Positions of the Li atoms in the FeV_3O_8 cavity: Li closed circles, oxygen open circles. (B) The five-coordinate lithium–oxygen square pyramid in $Li_2FeV_3O_8$. Lithium–oxygen bonds are shown as solid lines, and edges of the pyramid are shown as dashed lines. The lithium atom is only slightly out of the plane of the square face of the pyramid.

Bond lengths and angles for the final structural model of $Li_2FeV_3O_8$ are presented in Table IV. Due to the very low scattering power on the *M*1 site (primarily occupied by vanadium), the *M*1–oxygen distances obtained by NDPPA cannot be considered realistic. The *M*2–oxygen coordination (*M*2 is primarily occupied by iron) is a slightly distorted octahedron, with an average *M*2–oxygen separation of 1.98 Å, not significantly different from the *M*2–oxygen separation found in FeV_3O_8 of 1.96 Å. The *M*2–oxygen coordination of $Li_2FeV_3O_8$ is somewhat more regular than that in FeV_3O_8, as observed in Mossbauer effect measurements which have shown iron to remain Fe^{3+} during Li insertion, which is therefore accompanied by reduction of vanadium (*13*). The regularities of both the *M*1 and *M*2 octahedra are indicated by their oxygen–oxygen distances, which average 2.807 and 2.790 Å, respectively, in $Li_2FeV_3O_8$, slightly larger than the average separations of 2.73 and 2.77 Å reported for FeV_3O_8. The fivefold Li–O coordination is quite regular, with Li–O bond distances between 1.96 and 2.15 Å, (and O–Li–O angles close to those of an ideal octahedron) in very good agreement with Li–O bond distances reported for six coordinate Li ions in other ternary metal oxides. Lithium ions in the same perovskite-like cavity in $Li_2FeV_3O_8$ are 4.20(5) Å apart, and the nearest Li neighbor, in an adjacent cavity sharing one edge of the LiO_5 square pyramid, is located at a distance of 2.65(5) Å. This separation is much greater than that of the Li in face shared octahedra in Li_2ReO_3 (2.11(4) Å (2)) and larger also than that of the Li in Li_2O (2.31 Å). The relatively large Li temperature factor (Table III) may either be evidence of significant diffusion-like motion of Li at room temperature, or vibration of Li in a relatively flat potential well.

Discussion and Conclusions

We have found that FeV_3O_8 accommodates two Li per formula unit in a VO_2(B) type structure with minimal distortion of the host structure. Such lack of distortion is not surprising in structures where extensive *CS* is present, and is in strong contrast to the distortions in ReO_3 where the host is exclusively corner shared. In the structures with crystallographic shear the perovskite-like cavities are not extensively distorted on Li insertion, and therefore Li must be accommodated in coordination geometries already defined by the host. We have found

TABLE IV

BOND LENGTHS AND ANGLES FOR $Li_2FeV_3O_8$ (NEUTRON REFINEMENT CELL PARAMETERS: a = 11.9591(5), b = 3.9179(2), c = 6.4652(3), β = 107.228(3))

*M*1 octahedron		*M*2 octahedron		Li polyhedron	
*M*1–O2[a]	1.51(3)	*M*2–O3	1.86(1)	Li–O2	2.15(2)
*M*1–O3	1.89(3)	(2) *M*2–O4	1.97(1)	(2) Li–O3	1.963(1)
(2) *M*1–O2	2.02(1)	*M*2–O1	1.97(1)	Li–O4	1.99(2)
*M*1–O4	2.16(3)	*M*2–O3	2.02(1)	Li–O4	2.13(2)
*M*1–O1	2.54(3)	*M*2–O2	2.08(1)		
Avg	2.02	Avg	1.98	Avg	2.04
O1–O3	2.826(8)	O1–O2	3.001(8)	O2–O4	2.874(7)
O1–O4	2.876(6)	O1–O3	2.873(6)	O4–O4	3.151(8)
O2–O3	2.711(6)	O2–O3	2.711(6)	(2) O2–O3	2.859(5)
O2–O4	2.874(7)	O3–O3	2.594(11)	(2) O3–O4	2.809(4)
(2) O1–O2	2.873(5)	(2) O1–O4	2.797(5)	(2) O3–O4	2.848(5)
(2) O2–O2	2.770(6)	(2) O2–O4	2.699(5)		
(2) O3–O2	2.859(5)	(2) O3–O4	2.809(4)		
(2) O4–O2	2.699(5)	(2) O3–O4	2.848(5)		
Avg	2.807	Avg	2.790	Avg	2.882
O2–M1–O3	105.3(17)	O3–M2–O1	97.3(4)	O3–Li–O3	172.5(11)
(2) O2–M1–O2	102.4(7)	(2) O3–M2–O4	96.1(3)	(2) O3–Li–O4	92.3(7)
O2–M1–O4	101.7(12)	O3–M2–O3	83.8(4)	(2) O3–Li–O4	86.6(6)
O2–M1–O1	176.8(17)	O3–M2–O2	166.7(5)	(2) O3–Li–O2	88.0(7)
(2) O3–M1–O2	93.8(7)	(2) O1–M2–O4	90.5(2)	O4–Li–O4	99.9(10)
O3–M1–O4	153.0(15)	O1–M2–O3	179.0(5)	O4–Li–O2	175.6(12)
O3–M1–O1	77.9(8)	O1–M2–O2	96.0(4)	O4–Li–O2	84.5(7)
O2–M1–O2	151.1(17)	O4–M2–O4	167.6(6)		
(2) O2–M1–O4	80.3(9)	(2) O4–M2–O3	89.4(3)		
(2) O2–M1–O1	77.2(8)	(2) O4–M2–O2	83.8(3)		
O4–M1–O1	75.1(9)	O3–M2–O2	83.0(4)		

[a] The M1–O distances obtained by NDPPF are not considered realistic.

relatively regular square pyramidal five-coordinate sites to be occupied by Li in $Li_2FeV_3O_8$. Such sites are common to all *CS* structures based on ReO_3. In contrast, the Na in the Na_2TiO_2(B) bronze was found to occupy an eight-coordinate site at the center of the cavity (*14*). There are two additional five-coordinate square pyramidal sites present in each cavity in $Li_2FeV_3O_8$, which are not equivalent to the two occupied by Li. Refinements of Li occupancy in these sites showed them to be vacant. The approximate coordinates of the vacant sites are (0.85,0,0), best visualized in Fig. 3 by the equivalent position (0.35,0.5,0), approximately $\frac{1}{2}b$ below an O1 atom. These square pyramids share corners with those occupied by Li in $Li_2FeV_3O_8$, and have Li–O bond distances between 1.96 and 2.39 Å (average 2.08 Å). If all four sites in the cavity were to be occupied, no lithium ion would be less than 2.70 Å from its nearest Li neighbor. Based purely on geometrical and bond length considerations, then, accommodation of at least four Li per cavity is possible in VO_2(B) type structures, with resulting stoichiometry of one Li per host metal atom. These sites are probably partially occupied in $Li_{.75}VO_2$(B). For the reported inserted Li stoichiometry in nonstoichiometric V_6O_{13}, $Li_{7.6}V_6O_{13}$, 3.8 Li per triply capped perovskite cavity (see Fig. 1)

are required (*2*); 6 Li per formula unit can be accommodated in square pyramidal sites. In an undistorted V_2O_5 host, the double capped cavity (Fig. 1) allows the accommodation of one Li per host metal atom in square pyramidal sites.

Minimal distortion of the host structure and fivefold square pyramidal coordination of lithium in perovskite-like cavities are likely to be common in lithium inserted ReO_3 based *CS* structures such as those found for vanadium and niobium oxides in which the crystallographic shear defines ReO_3 blocks of finite size in two of three dimensions. Noncapped perovskite-like cavities occur in many *CS* structures within which neither octahedral nor square pyramidal sites are present. The host structure distortion which occurs for compounds such as $Li_{0.36}WO_3$(2), allowing the Li to assume square planar coordination, may not be possible in many *CS* structures. Structural studies of Li inserted *CS* structures of that type would therefore be of interest.

References

1. M. S. WHITTINGHAM, *Prog. Solid State Chem.* **12,** 41 (1978).
2. R. J. WISEMAN AND P. G. DICKENS, *J. Solid State Chem.* **17,** 91 (1976).
3. D. E. COX, R. J. CAVA, D. B. MCWHAN, AND D. W. MURPHY, *J. Phys. Chem. Solids* **43,** 657 (1982).
4. R. J. CAVA, A. SANTORO, D. W. MURPHY, S. ZAHURAK, AND R. S. ROTH, *J. Solid State Chem.* **42,** 251 (1982).
5. R. J. CAVA, A. SANTORO, D. W. MURPHY, S. ZAHURAK, AND R. S. ROTH, *Solid State Ionics* **5,** 323 (1981).
6. D. W. MURPHY, M. GREENBLATT, R. J. CAVA, AND S. M. ZAHURAK, *Solid State Ionics* **5,** 327 (1981).
7. R. MARCHAND, L. BROHAN, AND M. TOURNOUX, *Mater. Res. Bull.* **15,** 1129 (1980).
8. J. MULLER, J. C. JOUBERT, AND M. MAREZIO, *J. Solid State Chem.* **27,** 191 (1979).
9. H. M. RIETVELD, *J. Appl. Crystallogr.* **2,** 65 (1969).
10. E. PRINCE, "U. D. Tech. Note 1117 (F. J. Shorten, Ed.)," pp. 8–9, National Bureau of Standards, Washington, D.C. (1980).
11. A. SANTORO, R. J. CAVA, D. W. MURPHY, AND R. S. ROTH, "Neutron Scattering" (J. Faber, Ed.), Amer. Inst. of Phys. Conf. Proceed. nr. 89, p. 162 (1982).
12. G. E. BACON, *Acta. Crystallogr. Sect. A* **28,** 357 (1972).
13. M. EIBSCHUTZ, D. W. MURPHY, S. M. ZAHURAK, AND P. A. CHRISTIAN, *Solid State Ionics* **5,** 339 (1981).
14. S. ANDERSSON AND A. D. WADSLEY, *Acta. Crystallogr.* **15,** 201 (1962).